Globally Optimal Linear Approach for the Design of Process Equipment: The Case of Air Coolers

Priscila A. Souza and André L. H. Costa
Instituto de Química, Rio de Janeiro State University (UERJ), Rio de Janeiro, Brazil

Miguel J. Bagajewicz
School of Chemical, Biological and Materials Engineering, University of Oklahoma, Norman, OK 73019

DOI 10.1002/aic.15977
Published online October 20, 2017 in Wiley Online Library (wileyonlinelibrary.com)

In a recent article, Gonçalves et al., introduced a linear and rigorous methodology for equipment design, in particular shell-and-tube heat exchanger. Here, we explore its application to air coolers, a problem that we solve globally for the first time. Because the approach is linear, results are globally optimal. The objective function is the total annualized cost. The constraints include the thermal and hydraulic modeling of the process stream flow in the tube bundle and the air flow through the finned surface. In addition, we worked on reducing computing time, through an analysis of different alternatives for the description of the original discrete variables organized in sets of binary variables. The performance of the proposed approach is illustrated through its comparison with an air cooler described in the literature. © 2017 American Institute of Chemical Engineers *AIChE J*, 64: 886–903, 2018
Keywords: heat transfer, optimization

Introduction

The task of cooling streams using shell-and-tube heat exchangers and utilities is usually associated to the installation of a complete cooling water system, encompassing cooling towers, pumps, and a pipe network to distribute cooling water to the plant coolers and to return it to the cooling tower. The mechanism of cooling associated to a cooling tower implies water make-up to compensate for evaporation.[1] In arid regions or highly dense industrial areas, the water supply availability may be particularly limited. This problem may be even more severe in the future, where disturbances in the rainfall regime due to the climate change are expected.[2] The limitations imposed by water shortage in new projects or revamps can be mitigated by the substitution of shell-and-tube coolers by air coolers.

In air coolers, the hot process stream flows on the inside of a bundle of finned tubes and air is used to perform the cooling by flowing perpendicularly to the bundle of tubes. The flow of air outside the tube bundle is usually aided by fans as natural convection is not sufficient. Because the capital costs associated to air coolers are relatively higher and a process plant may have a large cooling demand, it is important to guarantee the best air cooler solution during the design of new units.

Despite its importance, the literature about the design optimization of air coolers is not as extended as that of shell-and-tube heat exchangers. The presence of fans in air coolers imposes that its operation demands energy consumption. Therefore, the typical formulation of the air cooler design optimization problem encompasses capital and operating costs, different from the case of shell-and-tube heat exchangers where the problem is commonly formulated in the literature as the minimization of the heat transfer area subject to maximum allowable pressure drops.[3]

Previous papers have solved the air cooler design problem using two different approaches: metaheuristic methods[4–7] and mathematical programming.[8,9] González et al.[8] formulated the design problem as a nonlinear programming (NLP). The thermohydraulic constraints are not explicitly stated in the formulation, but they are handled using a simulation code. The problem is solved using a sequential quadratic programming method. Doodman et al.[4] employed metaheuristic methods for solution of the air cooler design problem. The dimension of the problem is reduced using a global sensitivity analysis approach to identify the most important design variables to be included in the optimization. They compared harmony search and genetic algorithms, where the former identified a solution with a slightly smaller objective function. In turn, Karami et al.[5] employed the Imperialist Competitive Algorithm for the optimization of the installation of twisted tapes in air coolers for increasing the tube-side heat-transfer coefficient. This approach was also employed by the same authors in the analysis of butterfly inserts.[6] Kashani et al.[7] employed genetic algorithms to solve an air cooler design problem involving multiobjective optimization. The objective functions investigated were the temperature approach and the total annualized cost. Finally, Manassaldi et al.[9] formulated the design problem as a mixed-integer NLP (MINLP) aiming at the minimization of the total annualized cost, including capital and operating costs.

Additional Supporting Information may be found in the online version of this article.

Correspondence concerning this article should be addressed to M. J. Bagajewicz at bagajewicz@ou.edu

At best, all the aforementioned approaches identify local optimum designs. Therefore, there is a need to identify the best design, that is, one that qualifies mathematically as a global optimum. This is therefore the objective of this article.

Starting from one set of nonlinear design equations taken from Serth,[10] we take advantage of the fact that several parts are geometrically standardized using discrete values (e.g., tubes only come in certain finite set of standard diameters and lengths). This substitution leads to a mixed-integer nonlinear model that we rigorously reformulate as a mixed-integer linear programming (MILP), thus guaranteeing global optimality. The MILP computational effort is reduced through the analysis of different alternatives for the representation of the design variables using binary variables. This technique was employed successfully to the design of shell-and-tube heat exchangers and is explored here for air coolers.[11,12]

The article is organized as follows. We first present the nonlinear model taken from Serth.[10] Then, we describe the reformulation of the nonlinear model to obtain a linear optimization problems and present the objective function and constraints of the best alternative identified. After that, we present how convergence can be accelerated and, finally, we show the numerical results.

Mathematical Model

This section presents the problem parameters, variables, and the original nonlinear equations of the air cooler model. Aiming at making the presentation easier to the reader, the parameters are differentiated from the variables using the symbol "^" over them.

Problem parameters

The air cooler unit must cool a hot stream with mass flow rate $\hat{m}h$ from an inlet temperature $\hat{T}hi$ to an outlet temperature $\hat{T}ho$. Consequently, the heat load $\hat{Q}$ is fixed. The tube-side pressure drop must be lower than $\Delta\hat{P}max$ and the flow velocity must be higher than $\hat{v}hmin$ (avoiding excessive fouling) and lower than $\hat{v}hmax$ (avoiding erosion).

This cooling service is performed using an air mass flow rate $\hat{m}c$ with known inlet and outlet temperatures ($\hat{T}ci$ and $\hat{T}co$, respectively). Thus, the logarithmic mean temperature difference ($\Delta\hat{T}lm$) is fixed.

The physical properties of the hot stream are considered constant: density $\hat{\rho}h$, heat capacity $\hat{C}ph$, viscosity $\hat{\mu}h$, and thermal conductivity $\hat{k}h$, associated to a Prandtl number $\hat{\mathrm{P}}\mathrm{rh}$. The equivalent air physical properties are also considered constant: $\hat{\rho}c$, $\hat{C}pc$, $\hat{\mu}c$, and $\hat{k}c$, with a Prandtl number $\hat{P}rc$. A routine was implemented to determine the physical properties of the air automatically, before the optimization, using a temperature reference equivalent to the mean temperature between inlet and outlet, and correlations obtained using the results of a *PRO II* simulation[10]

$$\hat{T}cm=\frac{\hat{T}co+\hat{T}ci}{2} \tag{1}$$

$$\hat{\rho}c=1.4107.10^{-11}\hat{T}cm^4-2.1124.10^{-8}\hat{T}cm^3+1.2845.10^{-5}\hat{T}cm^2-4.5851.10^{-3}\hat{T}+1.2942 \tag{2}$$

$$\hat{k}c=-2.7221.10^{-8}\hat{T}cm^2+7.8051.10^{-5}\hat{T}cm+2.4134.10^{-2} \tag{3}$$

$$\hat{C}pc=-3.6649.10^{-7}\hat{T}cm^3+4.8370.10^{-4}\hat{T}cm^2+1.77.10^{-2}\hat{T}cm+1008.9 \tag{4}$$

$$\hat{\mu}c=3.7778.10^{-8}\hat{T}cm+1.7887.10^{-5} \tag{5}$$

The fouling factors of both streams are also fixed: $\hat{R}fh$ and $\hat{R}fc$. The material selection conducted before the optimization defines the thermal conductivity of the tube wall and fins, $\hat{k}t$ and $\hat{k}f$, respectively. The tube thickness is also previously established, $\hat{\delta}t$.

The fan system is characterized by a set of efficiencies involving the fan ($\hat{\eta}fan$), speed reducer ($\hat{\eta}sr$), and motor ($\hat{\eta}motor$). The electricity price for the fan operation is $\hat{C}en$ and the air cooler operates during $\hat{h}op$ hours per year. Finally, the economic analysis is based on an interest rate $\hat{i}$ and a project lifetime $\hat{y}$.

Design variables

The air cooler unit to be designed corresponds to a bank of bays, where each bay is formed by a set of tube bundles that are served by the same fan.[13] The design variables include the number of bays (*Nbay*), the number of bundles per bay (*Nbbay*), and the number of fans associated to each bay (*Nfanbay*). Figure 1 depicts an example of a bank of air coolers with three bays (*Nbay*=3), two bundles per bay (*Nbbay*=2), and two fans per bay (*Nfanbay*=2).

Every bundle is composed of a set of tubes distributed along a set of rows (*Nr*), where each row has a certain number of tubes (*Ntr*). The flow along these rows of tubes is defined according to the number of tube passes (*Npt*). Figure 2 shows a front view of a tube bundle with six rows (*Nr*=6), where each row has 23 tubes (*Ntr*=23).

The air cooler is built with finned tubes associated to the following design variables: tube length (*L*), outer and inner diameters of the root tube (*Dte* and *Dti*), fin height (*Lf*), fin thickness (*tf*), and number of fins per meter (*Nf*). The tubes are organized in the bundle in a triangular pattern and the tube pitch is a design variable represented by the tube pitch ratio (*rp*).

The air cooler fans are characterized by their diameter (*Dfan*). The selection between induced or forced draft depends on several aspects of the problem, for example, pipe rack installation, noise, and air recirculation.[14] Therefore, it is

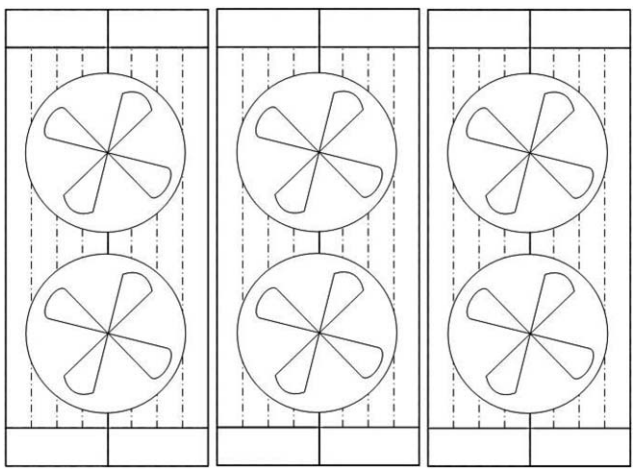

Figure 1. A bank with three bays of air coolers (upper view).

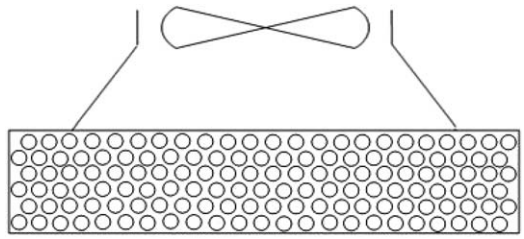

Figure 2. An air cooler bundle (front view).

considered that this decision is established prior to the optimization and it is out of the scope of the optimization.

Constraints

The constraints encompass the hot stream, air, and overall heat-transfer coefficient equations, the heat transfer area relations, the LMTD correction factor equations, the hot stream pressure drop and air flow power consumption, and the economic model for capital, maintenance, and operating costs. The thermofluidynamic model equations are formulated based on Serth,[10] complemented by an analysis of the LMTD correction factor based on the data published by Saunders.[14]

Hot stream heat-transfer coefficient

Assuming turbulent flow, the Nusselt number of the tube side where the hot stream flows (*Nuh*) and, consequently, the heat-transfer coefficient for the hot stream (*hh*) are based on the Seider and Tate correlation

$$Nuh = 0.023 Reh^{0.8} \hat{P}rh^{1/3} \tag{6}$$

$$hh = \frac{Nuh\ \hat{k}h}{Dti} \tag{7}$$

where *Reh* is the Reynolds number of the hot stream, which can be evaluated by the following expression

$$Reh = \frac{4Npt\ \hat{m}h}{\pi\ Dti\ Nbay\ Nbbay\ Ntr\ Nr\ \hat{\mu}h} \tag{8}$$

The validity of the Seider and Tate correlation is represented by the following constraints

$$Reh \geq 10,000 \tag{9}$$

$$\frac{L}{Dti} \geq 10 \tag{10}$$

Air stream heat-transfer coefficient

The Nusselt number of the air flow (*Nuc*) and, consequently, the heat-transfer coefficient (*hc*) are determined using the following correlation[10]

$$Nuc = 0.38 Rec^{0.6} \hat{P}rc^{1/3} (Aot/Ar)^{-0.15} \tag{11}$$

$$hc = \frac{Nuc\,\hat{k}c}{Dte} \tag{12}$$

where *Rec* is the Reynolds number of the air flow, *Ar* is the outside bare area per unit length, and *Aot* is the total finned surface area per unit length.

The expression for *Ar* evaluation is

$$Ar = \pi\, Dte \tag{13}$$

The total finned area *Aot* can be calculated by the sum of the exposed area of the root tube (*Ab*) and the fin area (*Aof*)

$$Aot = Ab + Aof \tag{14}$$

$$Ab = \pi\ Dte(1 - tf\ Nf) \tag{15}$$

$$Aof = 2Nf \frac{\pi}{4}\left(Df^2 - Dte^2\right) + \pi\ Df\ tf\ Nf \tag{16}$$

where *Df* is the fin diameter, given by

$$Df = Dte + 2Lf \tag{17}$$

The Reynolds number of the air flow is based on the velocity of the air stream through the minimum flow area (*vcmax*)

$$Rec = \frac{Dte\ vcmax\ \hat{\rho}c}{\hat{\mu}c} \tag{18}$$

The minimum flow area corresponds to the product of the total projection area of the air cooler (*Aface*) multiplied by the free-area ratio (*FAR*)

$$Aface = Nbay\ Nbbay\quad W\ L \tag{19}$$

$$FAR = 1 - \frac{Dte + 2Nf\ Lf\ tf}{Ltp} \tag{20}$$

where *W* is the bundle width

$$W = Ltp\ Ntr \tag{21}$$

Therefore

$$vcmax = \frac{\hat{m}c/\hat{\rho}c}{Aface\,FAR} \tag{22}$$

The validity of the correlation employed is represented by the following constraints

$$Nr \geq 3 \tag{23}$$

$$1800 \leq Rec \leq 10^5 \tag{24}$$

$$0.011176\ \text{m} \leq Dte \leq 0.0508\ \text{m} \tag{25}$$

$$0.00584\,\text{m} \leq Lf \leq 0.0191\,\text{m} \tag{26}$$

$$0.0274\,\text{m} \leq Ltp \leq 0.0986\,\text{m} \tag{27}$$

$$275 \leq Nf \leq 433 \tag{28}$$

$$1 \leq \frac{Aot}{Ar} \leq 50 \tag{29}$$

Finned surface overall efficiency (radial circular fin)

The overall efficiency of the finned surface (ηt) can be calculated using the fin efficiency and the geometry of the finned surface

$$\eta t = \left(\frac{Aot - Aof}{Aot}\right) + \eta f \left(\frac{Aof}{Aot}\right) \tag{30}$$

where ηf is the efficiency of an individual fin, that can be calculated by the following expressions

$$\eta f = \frac{\tanh(mf\ Lfe)}{mf\ Lfe} \tag{31}$$

$$mf = \left(\frac{2h'}{\hat{k}f\ tf}\right)^{0.5} \tag{32}$$

$$Lfe = Lf\left(1+\frac{tf}{2Lf}\right)\left[1+0.35\ln\left(\frac{Df}{Dte}\right)\right] \tag{33}$$

$$h' = \frac{hc}{1+\hat{R}fc\ hc} \tag{34}$$

The validity of these equations are

$$\frac{Lf}{tf} > 3 \tag{35}$$

$$\frac{Df}{Dte} < 3 \tag{36}$$

Overall heat-transfer coefficient

The expression of the overall heat-transfer coefficient (U) is

$$U = \frac{1}{\left(\frac{1}{hh}+\hat{R}fh\right)\left(\frac{Aot}{\pi\ Dti}\right)+\frac{Aot\ \ln\left(Dte/Dti\right)}{2\pi\ \hat{k}t}+\frac{1}{\eta t\ hc}+\frac{\hat{R}fc}{\eta t}} \tag{37}$$

Heat transfer area

The required heat transfer area ($Areq$) is calculated using the LMTD method

$$Areq = \frac{\hat{Q}}{U\ \Delta\hat{T}lm\ F} \tag{38}$$

where F is the correction factor of the LMTD.

To guarantee a reliable design of the air cooler, it is defined that the total heat transfer area (A) must be higher than the required area, associated to a design margin defined by the factor $\hat{X}a$

$$\hat{X}a \le \frac{A}{Areq} \tag{39}$$

Therefore, the required heat transfer area equation is reorganized and turns into a constraint based only on the total heat transfer area

$$UA \ge \hat{X}a\frac{\hat{Q}}{\Delta\hat{T}lm\,F} \tag{40}$$

Geometrically, the total heat transfer area depends on the number of bays ($Nbay$), the number of bundles per bay ($Nbbay$), the number of rows (Nr), the number of tubes per row (Ntr), the tube length (L), and the total finned surface area per unit length (Aot) as the following equations

$$A = Nbay\ Nbbay\ Nr\ Ntr\ Aot\ L \tag{41}$$

The description of the heat transfer area must be complemented by the following geometric constraints. The outer and the inner tube diameters are related to the tube thickness ($\hat{\delta}t$)

$$Dti = Dte - 2\hat{\delta}t \tag{42}$$

The fin spacing (sf) depends on the number of fins per unit length and the fin thickness

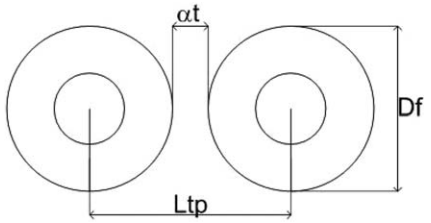

Figure 3. Finned tube spacing.

$$sf = \left(\frac{1}{Nf}\right) - tf \tag{43}$$

According to the definition of the tube pitch ratio, it yields

$$Ltp = Dte\ rp \tag{44}$$

The value of the tube pitch ratio must allow a minimum gap between adjacent fin tips, as shown in Figure 3

$$Ltp \ge Df + \hat{\alpha}t \tag{45}$$

LMTD correction factor

The LMTD correction factor depends on the air cooler configuration, represented by the number of passes (Npt) and number of tube rows (Nr). Here, the evaluation of the LMTD correction factor is based on the data displayed by Saunders.[14] In these data, the determination of the correction factor for each configuration ($\hat{F}conf$) depends on the value of the correction factor for the unmixed–unmixed cross-flow configuration ($\hat{F}base$). Since the end temperatures are previously known, this cross-flow correction factor is calculated before the optimization, using a procedure based on the P-NTU method[15]

$$\hat{F}base = \frac{\hat{\varepsilon}\left(\hat{T}hi-\hat{T}ci\right)}{\Delta\hat{T}lm\ N\hat{T}U} \tag{46}$$

where $N\hat{T}U$ is the number of transfer units and $\hat{\varepsilon}$ is the heat exchanger effectiveness

$$\hat{\varepsilon} = \frac{\hat{T}hi-\hat{T}ho}{\hat{T}hi-\hat{T}ci} \tag{47}$$

In turn $N\hat{T}U$ is related to $\hat{\varepsilon}$ as follows

$$\hat{\varepsilon} = 1-e^{\left[\left(\frac{1}{\hat{C}r}\right)\left(N\hat{T}U\right)^{0.22}\left\{e^{\left[-\hat{C}r\left(N\hat{T}U\right)^{0.78}\right]}-1\right\}\right]} \tag{48}$$

where $\hat{C}r$ is the ratio between heat capacity flow rates

$$\hat{C}r = \frac{\hat{m}h\,\hat{C}ph}{\hat{m}c\,\hat{C}pc} \tag{49}$$

Because Eq. 48 does not have an analytical solution for the determination of $N\hat{T}U$, its evaluation involves the application of a numerical method.

Table 1. LMTD Correction Factor for Air Coolers with One Tube Pass and *N* Tube Rows

Configuration	Mathematical Expression
One row per pass	$\hat{F}conf = 1.8\hat{F}base - 0.77$
Two rows per pass	$\hat{F}conf = 1.4\hat{F}base - 0.375$
Three rows per pass	$\hat{F}conf = 1.24\hat{F}base - 0.225$
Four rows per pass	$\hat{F}conf = 1.1\hat{F}base - 0.093$
More than five rows per pass	$\hat{F}conf = \hat{F}base$

Table 2. LMTD Correction Factor for Air Coolers with *N* Tube Passes and *N* Tube Rows

Configuration	Mathematical Expression
Two rows and two passes	$\hat{F}conf=-20\hat{F}base^3+49.86\hat{F}base^2-40.56\hat{F}base+11.65$
Three rows and three passes	$\hat{F}conf=-20\hat{F}base^3+50.14\hat{F}base^2-41.34\hat{F}base+12.17$
Four rows and four passes	$\hat{F}conf=-13.33\hat{F}base^3+32.57\hat{F}base^2-26.14\hat{F}base+7.87$
More than four rows and four passes	$\hat{F}conf=1$

The air cooler correction factor data published by Saunders[14] are organized in tables according to the cross-flow correction factor. Tables 1–3 show mathematical expressions obtained through the application of a curve fitting procedure over these data.

Tube-side pressure drop

Ignoring nozzle head losses, the tube-side pressure drop (ΔPh) takes into account the pressure drop caused by the fluid flow in the tubes (ΔPf) and the heads (ΔPr)

$$\Delta Ph=\Delta Pf+\Delta Pr \tag{50}$$

The pressure drop caused by the fluid flow inside the tubes is given by

$$\Delta Pf=\frac{fh\,Npt\,Gh^2L}{2\hat{\rho}h\,Dti^2} \tag{51}$$

where Gh is the mass flux of hot stream and fh is the friction factor.

The max flux is evaluated by the ratio between the mass flow rate and the total flow area in all tube bundles

$$Gh=\frac{\hat{m}h(Npt/Ntr\;\;Nr\;\;bay\;\;Nbbay)}{\pi\;\;Dti^2/4} \tag{52}$$

The expressions for the friction factor evaluation and its validity are

$$fh=0.4137Reh^{-0.2585} \tag{53}$$

$$Reh\geq 3000 \tag{54}$$

The heads pressure drop is

$$\Delta Pr=\frac{Gh^2\alpha r}{2\hat{\rho}h} \tag{55}$$

where αr depends on the number of tube passes

$$\alpha r=2Npt-1.5 \tag{56}$$

The total tube-side pressure drop must not be higher than the maximum allowed pressure drop

$$\Delta Ph\leq\Delta\hat{P}max \tag{57}$$

The tube-side flow velocity bounds are

$$\hat{v}hmin\leq\frac{Gh}{\hat{\rho}h}\leq\hat{v}hmax \tag{58}$$

Table 3. LMTD Correction Factor for Air Coolers with Two Tube Passes and Two Tube Rows with Fluid Mixing at the Header

Configuration	Mathematical Expression
Two rows and two passes	$\hat{F}conf=-0.86\hat{F}base^2+1.96\hat{F}base-0.106$

Fan power consumption

The air-side pressure drop (ΔPc) across the air cooler is given by

$$\Delta Pc=1.1\frac{2fc\,Gc^2Nr}{\hat{\rho}c} \tag{59}$$

where Gc is the air mass flux and fc is the friction factor.

The air mass flux is related to the flow velocity

$$Gc=\hat{\rho}c\,vcmax \tag{60}$$

The expression for evaluation of the friction factor is

$$fc=\left(1+\frac{2e^{-a/4}}{1+a}\right)\left(0.021+\frac{27.2}{Reeff}+\frac{0.29}{Reeff^{0.2}}\right) \tag{61}$$

where a and $Reeff$ are evaluated by

$$a=\frac{Ltp-Df}{Dte} \tag{62}$$

$$Reeff=Rec\frac{sf}{Lf} \tag{63}$$

The total air-side pressure variation must also consider the kinetic term

$$\Delta Pfan=\Delta Pc+\frac{\hat{\rho}c\;\;vfr^2}{2} \tag{64}$$

where vfr is the air velocity through the fans, calculated considering the air volumetric flow rate per fan ($qfan$)

$$vfr=\frac{qfan}{\frac{\pi}{4}Dfan^2} \tag{65}$$

$$qfan=\frac{\hat{m}c/\hat{\rho}cout}{Nbay\;\;Nfanbay} \tag{66}$$

The following constraints are used to impose that the area of the fans is at least 40% of the bay face area and that the fan diameters are properly circumvented in the bay limits, as shown in Figure 4

$$Nbbay\;\;W\geq Dfan+2\hat{f}d \tag{67}$$

$$Dfan+2\hat{f}l\leq L-Lfanp(Nfanbay-1) \tag{68}$$

$$\frac{\pi}{4}Nfanbay\;\;Dfan^2\geq 0.4Nbbay\;\;WL \tag{69}$$

where $\hat{f}l$ and $\hat{f}d$ are the minimum distances between the fan and the bay length and width, respectively.

Another geometric constraint involving the fan dimensions establishes the distance between the fan centers ($Lfanp$)

$$Lfanp=1.1Dfan \tag{70}$$

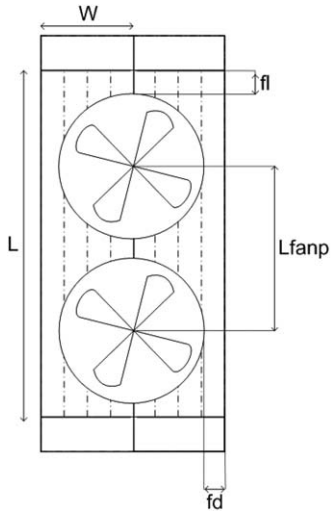

Figure 4. Fans arrangement (upper view).

The total pressure variation and the volumetric flow rate determine the power consumption per fan (*Wused*), together with the respective efficiencies of the fan, speed reducer, and motor

$$Wused = \frac{\Delta Pfan \;\; qfan}{1000 \;\; \hat{\eta}fan \;\; \hat{\eta}sr \;\; \hat{\eta}motor} \tag{71}$$

Economic model

The economic model is based on the proposal of Conradie et al.[16] The air cooler total annualized cost takes into account capital, maintenance, and operational costs.

The capital cost (*Cinv*) includes both finned tube bundle cost (*Che*) and the fan system investment cost (*Cfs*)

$$\begin{aligned} Che = Ntr \;\; Nr \;\; Nbay \;\; Nbbay \;\; \{[10010\left(Dte^2 - Dti^2\right) \\ + 17193\left(Df^2 - Dte^2\right)Nf \;\; tf + 1.27DteNf + 4.06]L + 32.5\} \end{aligned} \tag{72}$$

$$Cfs = Nfanbay \;\; Nbay\left(1887.5 + 163.49Dfan^2 + 281.25Wused\right) \tag{73}$$

$$Cinv = Che + Cfs \tag{74}$$

The yearly maintenance cost (*Cmai*) is defined as a percentage of the finned tube bundle cost and the fan system cost

$$Cmai = 0.01Che + 0.03Cfs \tag{75}$$

The operational cost (*Cop*) depends on the electrical power consumed per fan (*Wused*), the electricity price ($\hat{C}en$), and the number of operating hours per year ($\hat{h}op$)

$$Cop = \hat{h}op \;\; \hat{C}en \;\; Wused \;\; Nbay \;\; Nfanbay \tag{76}$$

Objective function

The *TAC* (total annualized cost) is used as objective function and it is computed by the following equation

$$TAC = C\hat{R}F \;\; Cinv + Cmai + Cop \tag{77}$$

where $C\hat{R}F$ is the capital recovery factor

$$C\hat{R}F = \frac{\hat{i}\left(1+\hat{i}\right)\hat{y}}{\left(1+\hat{i}\right)\hat{y}} - 1 \tag{78}$$

Discrete representation of geometric variables

All the design variables mentioned above are defined according to a set of standard values. Therefore, these variables can be represented by sets of binary variables. Thus, each discrete variable (x) is represented according to its respective indexed values ($\hat{x}d_i$) and only one of the listed indexed values can be selected. The selection of the indexed value is made using binary variables (y_i) as the following example

$$x = \sum_{i=1}^{imax} \hat{x}d_i y_i \tag{79}$$

$$\sum_{i=1}^{imax} y_i = 1 \tag{80}$$

The application of this structure to the air cooler variables is described below. Due to its nature, the finned surface and the heat exchanger configuration relates more than one discrete variable to the same set of binary variables.

Finned surface. The commercial alternatives of the finned surface involve different options of root tube diameter, fin height and thickness, and number of fins per meter. Therefore, these variables are originally controlled by the same set of binaries

$$Dte = \sum\nolimits_{stube=1}^{stubemax} p\hat{D}te_{stube} ytube_{stube} \tag{81}$$

$$Lf = \sum\nolimits_{stube=1}^{stubemax} p\hat{L}f_{stube} ytube_{stube} \tag{82}$$

$$Nf = \sum\nolimits_{stube=1}^{stubemax} p\hat{N}f_{stube} ytube_{stube} \tag{83}$$

$$tf = \sum\nolimits_{stube=1}^{stubemax} p\hat{t}f_{stube} ytube_{stube} \tag{84}$$

$$\sum\nolimits_{stube=1}^{stubemax} ytube_{stube} = 1 \tag{85}$$

Tube length.

$$L = \sum\nolimits_{sL=1}^{sLmax} p\hat{L}_{sL} yL_{sL} \tag{86}$$

$$\sum\nolimits_{sL=1}^{sLmax} yL_{sL} = 1 \tag{87}$$

Tube pitch ratio.

$$rp = \sum\nolimits_{srp=1}^{srpmax} p\hat{r}p_{srp} yrp_{srp} \tag{88}$$

$$\sum\nolimits_{srp=1}^{srpmax} yrp_{srp} = 1 \tag{89}$$

Number of bays.

$$Nbay = \sum\nolimits_{sNbay=1}^{sNbaymax} p\hat{N}bay_{sNbay} yNbay_{sNbay} \tag{90}$$

$$\sum\nolimits_{sNbay=1}^{sNbaymax} yNbay_{sNbay} = 1 \tag{91}$$

Number of bundles per bay.

$$Nbbay = \sum\nolimits_{sNbbay=1}^{sNbbaymax} p\hat{N}bbay_{sNbbay} yNbbay_{sNbbay} \tag{92}$$

$$\sum_{sNbbay=1}^{sNbbaymax} yNbbay_{sNbbay}=1 \tag{93}$$

Number of tubes per row.

$$Ntr=\sum_{sNtr=1}^{sNtrmax} p\hat{N}tr_{sNtr}yNtr_{sNtr} \tag{94}$$

$$\sum_{sNtr=1}^{sNtrmax} yNtr_{sNtr}=1 \tag{95}$$

Air cooler configuration and LMTD correction factor. The number of rows, tube passes, and correction factor are interrelated, thus they share the same set of binaries

$$Nr=\sum_{sconf=1}^{sconfmax} p\hat{N}r_{sconf}yconf_{sconf} \tag{96}$$

$$Npt=\sum_{sconf=1}^{sconfmax} p\hat{N}pt_{sconf}yconf_{sconf} \tag{97}$$

$$F=\sum_{sconf=1}^{sconfmax} \hat{F}conf_{sconf}yconf_{sconf} \tag{98}$$

$$\sum_{sconf=1}^{sconfmax} yconf_{sconf}=1 \tag{99}$$

Number of fans per bay.

$$Nfanbay=\sum_{sNfanbay=1}^{sNfanbaymax} p\hat{N}fanbay_{sNanfbay}yNfanbay_{sNanfbay} \tag{100}$$

$$\sum_{sNfanbay=1}^{sNfanbaymax} yNfanbay_{sNfanbay}=1 \tag{101}$$

Fan diameter.

$$Dfan=\sum_{sDfan=1}^{sDfanmax} p\hat{D}fan_{sDfan}yDfan_{sDfan} \tag{102}$$

$$\sum_{sDfan=1}^{sDfanmax} yDfan_{sDfan}=1 \tag{103}$$

Reformulation as a Linear Model

The development of the MILP formulation from the original nonlinear model involves the following steps: (1) aggregation of the binary variables, (2) organization of the data table, (3) model reformulation, and (4) conversion to a linear model.

Aggregation of binary variables

As shown above, the original representation of the discrete variables employs sets of binary variables according to the nature of the corresponding variable. However, the combination of the discrete values in tables yields other forms of representation using binaries. In this case, different groups of discrete variables are represented by the same set of binary variables. Table 4 describes three alternatives of aggregations explored in this article. Alternative 1 corresponds to the original aggregation described above, as performed by Gonçalves et al.[11] Alternative 3 is the maximum aggregation status, where a unique set of binaries is employed to describe all discrete variables and it is the alternative presented by Gonçalves et al.[12] Alternative 2 is an intermediate scheme. Each alternative presents a different computational performance. Because Alternative 3 presented the best performance in the numerical tests, this option will be described in detail next. The derivations of the other alternatives are available in the supporting information.

Organization of the data table

The original MINLP problem contains several sets of standard values of the discrete variables ($\hat{x}d_i$) shown in Eqs. 81–103. In Alternative 3, all these values are identified by a unique set of binaries (*yrow*) using a multi-index *srow*

$$srow=(sconf, sDfan, sL, sNbay, sNbbay, sNfanbay, sNtr, srp, stube) \tag{104}$$

Therefore, the identification of the standard values of the discrete variables is reorganized in a multi-indexed table, as follows

$$P\hat{D}te_{srow}=p\hat{D}te_{stube} \tag{105}$$

$$P\hat{L}f_{srow}=p\hat{L}f_{stube} \tag{106}$$

$$P\hat{N}f_{srow}=p\hat{N}f_{stube} \tag{107}$$

$$P\hat{t}f_{srow}=p\hat{t}f_{stube} \tag{108}$$

$$P\hat{L}_{srow}=p\hat{L}_{sL} \tag{109}$$

$$P\hat{r}p_{srow}=p\hat{r}p_{srp} \tag{110}$$

$$P\hat{N}bay_{srow}=p\hat{N}bay_{sNbay} \tag{111}$$

$$P\hat{N}bbay_{srow}=p\hat{N}bbay_{sNbbay} \tag{112}$$

$$P\hat{N}tr_{srow}=p\hat{N}tr_{sNtr} \tag{113}$$

$$P\hat{N}r_{srow}=p\hat{N}r_{sconf} \tag{114}$$

$$P\hat{N}pt_{srow}=p\hat{N}pt_{sconf} \tag{115}$$

$$P\hat{F}conf_{srow}=\hat{F}conf_{sconf} \tag{116}$$

$$P\hat{N}fanbay_{srow}=p\hat{N}fanbay_{sNanfbay} \tag{117}$$

$$P\hat{D}fan_{srow}=p\hat{D}fan_{sDfan} \tag{118}$$

Table 4. Alternatives Investigated for the Binary Variables Organization

Alternative	Binary Variable {Original Discrete Variable}
1	$ytube_{stube}$ {*Dte*, *Lf*, *Nf*, *tf*}, yL_{sL} {*L*}, yrp_{srp} {*rp*}, $yNbay_{sNbay}$ {*Nbay*}, $yNbbay_{sNbbay}$ {*Nbbay*}, $yNtr_{sNtr}$ {*Ntr*}, $yconf_{sconf}$ {*Nr*, *Npt*, *F*}, $yNfanbay_{sNfanbay}$ {*Nfanbay*}, $yDfan_{sDfan}$ {*Dfan*}
2	$yrowA_{srowA}$ {*Dte*, *Lf*, *Nf*, *tf*, *rp*}, $yrowB_{srowB}$ {*Nr*, *Npt*, *F*, *Ntr*}, $yrowC_{srowC}$ {*Nbay*, *Nbbay*}, $yrowD_{srowD}$ {*Nfanbay*, *Dfan*}, yL_{sL} {*L*}
3	$yrow_{srow}$ {*Dte*, *Lf*, *Nf*, *tf*, *L*, *rp*, *Nbay*, *Nbbay*, *Ntr*, *Nr*, *Npt*, *F*, *Nfanbay*, *Dfan*}

After the reorganization, the relation between the discrete variables and the binaries becomes

$$\sum_{srow} yrow_{srow} = 1 \tag{119}$$

$$Dte = \sum_{srow} P\hat{D}te_{srow} yrow_{srow} \tag{120}$$

$$Lf = \sum_{srow} P\hat{L}f_{srow} yrow_{srow} \tag{121}$$

$$Nf = \sum_{srow} P\hat{N}f_{srow} yrow_{srow} \tag{122}$$

$$tf = \sum_{srow} P\hat{t}f_{srow} yrow_{srow} \tag{123}$$

$$L = \sum_{srow} P\hat{L}_{srow} yrow_{srow} \tag{124}$$

$$rp = \sum_{srow} \mathrm{P}\hat{r}p_{srow} yrow_{srow} \tag{125}$$

$$Nbay = \sum_{srow} P\hat{N}bay_{srow} yrow_{srow} \tag{126}$$

$$Nbbay = \sum_{srow} P\hat{N}bbay_{srow} yrow_{srow} \tag{127}$$

$$Ntr = \sum_{srow} P\hat{N}tr_{srow} yrow_{srow} \tag{128}$$

$$Nr = \sum_{srow} P\hat{N}r_{srow} yrow_{srow} \tag{129}$$

$$Npt = \sum_{srow} P\hat{N}pt_{srow} yrow_{srow} \tag{130}$$

$$F = \sum_{srow} P\hat{F}conf_{srow} yrow_{srow} \tag{131}$$

$$Nfanbay = \sum_{srow} P\hat{N}fanbay_{srow} yrow_{srow} \tag{132}$$

$$Dfan = \sum_{srow} P\hat{D}fan_{srow} yrow_{srow} \tag{133}$$

Model reformulation

The problem reformulation consists in the substitution of the discrete variables by the respective binary representation in all equations of the model. This reformulation procedure also involves the rearrangement procedure presented below.

Let B be a variable which is a function of two or more discrete variable $C, D, \ldots, Z$, as follows

$$B = C^c D^d (\ldots) Z^z \tag{134}$$

After the substitution of all binary representations, it yields ($i, j, \ldots, k$ can be a multi-index)

$$B = \left(\sum_i P\hat{C}_i yC_i \right)^c \left(\sum_j P\hat{D}_j yD_j \right)^d (\ldots) \left(\sum_k P\hat{Z}_k yZ_k \right)^z \tag{135}$$

However, because the binary variables assume a value 1 only once in the corresponding set, this equation can be simplified

$$B = \sum_{i,j,\ldots,k} \left(P\hat{C}_i\right)^c \left(P\hat{D}_j\right)^d (\ldots) \left(P\hat{Z}_k\right)^z yC_i yD_j yZ_k \tag{136}$$

Therefore, after this procedure, the model equations become composed of expressions containing multiple summations of products of binary variables. Particularly, for Alternative 3, where there is only one set of binaries, this expression becomes even simpler

$$B = \sum_{srow} \left(P\hat{C}_{srow}{}^c P\hat{D}_{srow}{}^d (\ldots) P\hat{Z}_{srow}{}^z \right) y_{srow} \tag{137}$$

Conversion to a linear model

The substitution of the product of binaries in Eq. 136 by a nonnegative variable $w_{i,j,\ldots,k}$ yields

$$B = \sum_{i,j,\ldots,k} \left(P\hat{C}_i\right)^c \left(P\hat{D}_j\right)^d (\ldots) \left(P\hat{Z}_k\right)^z w_{i,j,\ldots,k} \tag{138}$$

The nonlinearity associated to the relation between the new variable $w_{i,j,\ldots,k}$ and its binary variables can be eliminated using a set of linear inequalities

$$w_{i,j,\ldots,k} \leq yC_i \tag{139}$$

$$w_{i,j,\ldots,k} \leq yD_j \tag{140}$$

$$w_{i,j,\ldots,k} \leq yZ_k \tag{141}$$

$$w_{i,j,\ldots,k} \geq yC_i + yD_j + \cdots + yZ_k - (m-1) \tag{142}$$

where m is the number of binary variables associated to the variable $w_{i,j,\ldots,k}$. For Alternative 3, this step is not necessary because there is only one set of binary variables (i.e., there is no product of variables in Eq. 137). This aspect of Alternative 3 implies in an integer linear programming problem (ILP).

Linear Formulation for Alternative 3

This section presents the development of the formulation associated to the Alternative 3, resultant from the application of the procedure described above.

The constraints related to bounds on discrete variables selected by the mathematical model (Eqs. 23 and 25–28) are not present in the final model, because it is possible to select previously the discrete values of the search space to respect the correlations imposed limits.

Hot stream heat-transfer coefficient

The substitution of the binary variables in Eq. 8 yields the following representation of the hot stream Reynolds number

$$Reh = \sum_{srow} P\hat{R}eh_{srow} yrow_{srow} \tag{143}$$

where

$$P\hat{R}eh_{srow} = \frac{4\hat{m}h}{\pi \hat{\mu} h} \frac{P\hat{N}pt_{srow}}{\left(P\hat{D}te_{srow} - 2\hat{\delta}t\right) P\hat{N}bay_{srow} P\hat{N}bbay_{srow} P\hat{N}tr_{srow} P\hat{N}r_{srow}} \tag{144}$$

This representation of the Reynolds number can be substituted in the Nusselt number expression in Eq. 6 and then in Eq. 7, thus yielding the expression of the heat-transfer coefficient in terms of the binary variables

$$hh=\sum_{srow} P\hat{h}h_{srow}yrow_{srow} \tag{145}$$

where

$$P\hat{h}h_{srow}=\hat{k}h\frac{P\hat{N}uh_{srow}}{P\hat{D}te_{srow}-2\hat{\delta}t} \tag{146}$$

$$P\hat{N}uh_{srow}=0.023\hat{P}rh^{1/3}\left(P\hat{R}eh_{srow}\right)^{0.8} \tag{147}$$

The validity of the Seider and Tate correlation represented by Eqs. 9 and 10 becomes

$$Re\hat{h}min \le \sum_{srow1} PRe\hat{h}_{srow}yrow_{srow} \tag{148}$$

$$\sum_{srow}\frac{P\hat{L}_{srow}}{P\hat{D}te_{srow}-2\hat{\delta}t}yrow_{srow} \ge 10 \tag{149}$$

Air stream heat-transfer coefficient

The representation of the air stream heat-transfer coefficient in binaries depends on the reorganization of the air velocity equation (*vcmax*), the outside bare area per unit length (*Ar*), and the total finned surface area per unit length (*Aot*).

The representation of the air velocity in the bundle can be obtained through the substitution of the binary variables in Eqs. 19–22

$$vcmax=\sum_{srow} P\hat{v}cmax_{srow}yrow_{srow} \tag{150}$$

where

$$P\hat{v}cmax_{srow}=\left(\frac{\hat{Q}}{\hat{\rho}c\ \hat{C}pc\left(\hat{T}co-\hat{T}ci\right)}\right)\left(\frac{1}{\left(\hat{Pr}p_{srow}P\hat{D}te_{srow}-P\hat{D}te_{srow}-2P\hat{N}f_{srow}P\hat{L}f_{srow}P\hat{t}f_{srow}\right)P\hat{N}bay_{srow}P\hat{N}bbay_{srow}P\hat{L}_{srow}P\hat{N}tr_{srow}}\right) \tag{151}$$

Then, the air stream Reynolds number, previously defined by Eq. 18, turns into

$$Re\,c=\sum_{srow} P\hat{R}ec_{srow}yrow_{srow} \tag{152}$$

where

$$P\hat{R}ec_{sNbay,sNbbay,sL,sNtr,srLtp,stube}=\left(\frac{\hat{Q}}{\hat{\mu}c\,\hat{C}pc\left(\hat{T}co-\hat{T}ci\right)}\right)\left(\frac{P\hat{D}te_{srow}}{\left(P\hat{r}p_{srow}P\hat{D}te_{srow}-P\hat{D}te_{srow}-2P\hat{N}f_{srow}P\hat{L}f_{srow}P\hat{t}f_{srow}\right)P\hat{N}bay_{srow}P\hat{N}bbay_{srow}P\hat{L}_{srow}P\hat{N}tr_{srow}}\right) \tag{153}$$

The substitution of the binary variables in the outside bare area per unit length (Eq. 13) and the total finned surface area per unit length (Eq. 14) yields

$$Ar=\pi\sum_{srow} P\hat{D}te_{srow}yrow_{srow} \tag{154}$$

$$Aot=\sum_{srow} P\hat{A}ot_{srow}yrow_{srow} \tag{155}$$

where

$$P\hat{A}ot_{srow}=\pi\left[P\hat{D}te_{srow}+2P\hat{N}f_{srow}P\hat{L}f_{srow}\left(P\hat{D}te_{srow}+P\hat{L}f_{srow}+P\hat{t}f_{srow}\right)\right] \tag{156}$$

Based on these expressions, the representation of the Nusselt number in binaries can be obtained through the substitution of Eqs. 152, 154, and 155 in Eq. 11. Finally, the binary representation of the air stream heat-transfer coefficient is obtained through Eq. 12

$$hc=\sum_{srow} P\hat{h}c_{srow}yrow_{srow} \tag{157}$$

where

$$P\hat{h}c_{srow}=\hat{k}c\frac{P\hat{N}uc_{srow}}{P\hat{D}te_{srow}} \tag{158}$$

$$P\hat{N}uc_{srow}=0.38\hat{P}rc^{1/3}\left(P\hat{R}ec_{srow}\right)^{0.6}\left(P\hat{A}ot_{srow}/\pi P\hat{D}te_{srow}\right)^{-0.15} \tag{159}$$

The validity of the correlation expressed in Eq. 24 can be reformulated using the binary representation of the Reynolds number in Eq. 152

$$Re\hat{c}min \le \sum_{srow} P\hat{R}ec_{srow}yrow_{srow} \le Re\hat{c}max \tag{160}$$

According to the relation between the pitch ratio, the tube pitch, and the tube outer diameter represented by Eq. 44, the bound on the tube pitch in Eq. 27 turns into

$$0.0274\,\mathrm{m} \le \sum_{srow} P\hat{D}te_{srow}\hat{Pr}p_{srow}yrow_{srow} \le 0.0986\,\mathrm{m} \tag{161}$$

The constraint in Eq. 29 is reorganized using Eqs. 154 and 155

$$1 \le \sum_{srow} \frac{P\hat{A}ot_{srow}}{\pi P\hat{D}te_{srow}} yrow_{srow} \le 50 \tag{162}$$

Finned surface overall efficiency (radial circular fin)

The reorganization of the overall efficiency of the finned surface (ηt) depends on the efficiency of an individual fin (ηf), the total finned surface area per unit length (Aot), and the fin area (Aof).

The substitution of the discrete variables in Eqs. 32–34 and then in Eq. 31 gives the new equation for the efficiency of an individual fin

$$\eta f = \sum_{srow} P\hat{\eta}f_{srow} yrow_{srow} \tag{163}$$

where

$$P\hat{\eta}f_{srow} = \frac{\tanh\left(P\hat{m}f_{srow} P\hat{L}fe_{srow}\right)}{P\hat{m}f_{srow} P\hat{L}fe_{srow}} \tag{164}$$

$$P\hat{L}fe_{srow} = P\hat{L}f_{srow}\left(1+\frac{P\hat{t}f_{srow}}{2P\hat{L}f_{srow}}\right)\left[1+0.35\ln\left(\frac{P\hat{D}te_{srow}+2P\hat{L}f_{srow}}{P\hat{D}te_{srow}}\right)\right] \tag{165}$$

$$P\hat{m}f_{srow} = \left[\frac{2P\hat{h}c_{srow}}{\hat{k}f\left(1+Rfc\,P\hat{h}c_{srow}\right)P\hat{t}f_{srow}}\right]^{0.5} \tag{166}$$

The substitution of the binary variables in Eq. 16 yields the new representation of Aof

$$Aof = \sum_{srow} P\hat{A}of_{srow} yrow_{srow} \tag{167}$$

where

$$P\hat{A}of_{srow} = \pi[2P\hat{N}f_{srow} P\hat{L}f_{srow}\left(P\hat{D}te_{srow}+P\hat{L}f_{srow}+P\hat{t}f_{srow}\right) + P\hat{D}te_{srow} P\hat{t}f_{srow} P\hat{N}f_{srow}] \tag{168}$$

Then, the substitution of Eqs. 163, 167, and 155 in Eq. 30 gives the new equation for ηt in binaries, which is

$$\eta t = \sum_{srow} P\hat{\eta}t_{srow} yrow_{srow} \tag{169}$$

where

$$P\hat{\eta}t_{srow} = \left(\frac{P\hat{A}ot_{srow}-P\hat{A}of_{srow}}{P\hat{A}ot_{srow}}\right)+P\hat{\eta}f_{srow}\left(\frac{P\hat{A}of_{srow}}{P\hat{A}ot_{srow}}\right) \tag{170}$$

The validity of these equations is now

$$\sum_{srow} \frac{P\hat{L}f_{srow}}{P\hat{t}f_{srow}} yrow_{srow} \ge 3 \tag{171}$$

$$\sum_{srow} \frac{P\hat{D}te_{srow}+2P\hat{L}f_{srow}}{P\hat{D}te_{srow}} yrow_{srow} \le 3 \tag{172}$$

Overall heat-transfer coefficient

The substitution of Eqs. 145, 155, 157, and 169 in Eq. 37 yields the binary representation of the overall heat-transfer coefficient

$$\frac{1}{U} = \sum_{srow} \frac{1}{P\hat{U}_{srow}} yrow_{srow} \tag{173}$$

where

$$\frac{1}{P\hat{U}_{srow}} = \left(\frac{1}{P\hat{h}h_{srow}}+R\hat{f}h\right)\left[\frac{P\hat{A}ot_{srow}}{\pi\left(P\hat{D}te_{srow}-2\hat{\delta}t\right)}\right] + \left\{\frac{1}{2\pi\hat{k}t} P\hat{A}ot_{srow} \ln\left[\frac{P\hat{D}te_{srow}}{\pi\left(P\hat{D}te_{srow}-2\hat{\delta}t\right)}\right]\right\} + \left(\frac{1}{P\hat{\eta}t_{srow} P\hat{h}c_{srow}}\right)\left(\frac{R\hat{f}c}{P\hat{\eta}t_{srow}}\right) \tag{174}$$

Heat transfer area

The new equation of the heat transfer area is obtained through the substitution of the binary variables and the Aot expression from Eq. 155 in Eq. 41, thus yielding

$$A = \sum_{srow} P\hat{A}_{srow}\, yrow_{srow} \tag{175}$$

where

$$P\hat{A}_{srow} = P\hat{N}bay_{srow} P\hat{N}bbay_{srow} P\hat{N}r_{srow} P\hat{N}tr_{srow} P\hat{L}_{srow} P\hat{A}ot_{srow} \tag{176}$$

The constraint of the heat transfer equation in Eq. 40 is reorganized through the substitution of Eq. 98 of the LMTD correction factor, Eq. 173 of the overall heat-transfer coefficient, and Eq. 175 of the heat transfer area

$$\frac{\Delta\hat{T}lm}{\hat{X}a}\sum_{srow} P\hat{A}_{srow} P\hat{F}conf_{srow} yrow_{srow} \ge \hat{Q}\sum_{srow}\frac{1}{P\hat{U}_{srow}} yrow_{srow} \tag{177}$$

According to the discrete variables substitution in Eq. 45, the minimum gap between adjacent fin tips, which limits the pitch ratio is now

$$\sum_{srow} \hat{\mathrm{Pr}}p_{srow} P\hat{D}te_{srow} yrow_{srow} \ge \sum_{srow}\left(P\hat{D}te_{srow}+2P\hat{L}f_{srow}+\hat{\alpha}t\right) yrow_{srow} \tag{178}$$

Tube-Side Pressure Drop. After the substitution of the discrete variables in Eq. 52, the tube-side mass flux is now

$$Gh = \sum_{srow} P\hat{G}h_{srow} yrow_{srow} \tag{179}$$

where

$$P\hat{G}h_{srow} = \frac{4\hat{m}h}{\pi}\frac{P\hat{N}pt_{srow}}{P\hat{N}tr_{srow} P\hat{N}r_{srow} P\hat{N}bay_{srow} P\hat{N}bbay_{srow}\left(P\hat{D}te_{srow}-2\hat{\delta}t\right)^2} \tag{180}$$

The substitutions of the hot stream Reynolds number equation represented now by Eq. 143 in Eq. 53 of the friction factor and, then, the substitution of its result with Eq. 179 in Eq. 51 gives the new ΔPf equation

$$\Delta Pf = \sum_{srow} P\hat{D}Pf_{srow}\, yrow_{srow} \tag{181}$$

where

$$P\hat{D}Pf_{srow} = \frac{0.4137}{2\hat{\rho}h}\left(\frac{4\hat{m}h}{\pi\hat{\mu}h}\right)^{1.7415} \frac{P\hat{L}_{srow}\left(P\hat{N}pt_{srow}\right)^{2.7415}}{\left(P\hat{N}bay_{srow}P\hat{N}bbay_{srow}P\hat{N}tr_{srow}P\hat{N}r_{srow}\right)^{1.7415}\left(P\hat{D}te_{srow}-2\hat{\delta}t\right)^{4.7415}} \tag{182}$$

The new expression of ΔPr is obtained through the substitution of the discrete variables in Eq. 56 and then its substitution with Eq. 179 in Eq. 55

$$\Delta Pr = \sum_{srow} PD\hat{\mathrm{P}}\mathrm{r}_{srow} yrow_{srow} \tag{183}$$

where

$$PD\hat{P}r_{srow} = \frac{1}{2\hat{\rho}h}\left(\frac{4\hat{m}h}{\pi}\right)^{2} \frac{\left(P\hat{N}pt_{srow}\right)^{2}\left(2P\hat{N}pt_{srow}-1.5\right)}{\left[P\hat{N}bay_{srow}P\hat{N}bbay_{srow}P\hat{N}tr_{srow}P\hat{N}r_{srow}\left(P\hat{D}te_{srow}-2\hat{\delta}t\right)^{2}\right]^{2}} \tag{184}$$

The substitution of Eqs. 181 and 183 in Eq. 50 gives the total tube-side pressure drop

$$\Delta Ph = \sum_{srow}\left(P\hat{D}Pf_{srow}+PD\hat{\mathrm{P}}\mathrm{r}_{srow}\right) yrow_{srow} \tag{185}$$

The maximum allowed pressure drop constraint defined in Eq. 57 is now

$$\sum_{srow}\left(P\hat{D}Pf_{srow}+PD\hat{\mathrm{P}}\mathrm{r}_{srow}\right) yrow_{srow} \le \Delta\hat{\mathrm{P}}max \tag{186}$$

The tube-side flow velocity bounds described by Eq. 58 becomes

$$\hat{v}hmin \le \frac{1}{\hat{\rho}h}\sum_{srow} P\hat{G}h_{srow}\, yrow_{srow} \le \hat{v}hmax \tag{187}$$

Fan power consumption

The substitution of the discrete variables in Eqs. 61–63 gives the new equation of the air flow friction factor

$$fc = \sum_{srow} P\hat{f}c_{srow}\, yrow_{srow} \tag{188}$$

where

$$P\hat{f}c_{srow} = \left[1+\frac{2\exp\left(-P\hat{a}_{srow}/4\right)}{1+P\hat{a}_{srow}}\right]\left[0.021+\frac{27.2}{P\hat{R}eeff_{srow}}+\frac{0.29}{\left(P\hat{R}eeff_{srow}\right)^{0.2}}\right] \tag{189}$$

$$P\hat{a}_{srow} = P\hat{r}p_{srow} - \frac{P\hat{D}te_{srow}+2P\hat{L}f_{srow}}{P\hat{D}te_{srow}} \tag{190}$$

$$P\hat{R}eeff_{srow} = \left(\frac{1}{P\hat{N}f_{srow}} - P\hat{t}f_{srow}\right)\frac{P\hat{R}ec_{srow}}{P\hat{L}f_{srow}} \tag{191}$$

The substitution of Eq. 150 in Eq. 60 gives the new equation of the air flux flow

$$Gc = \sum_{srow} P\hat{G}c_{srow} yrow_{srow} \tag{192}$$

where

$$P\hat{G}c_{srow} = \hat{\rho}c\, P\hat{v}cmax_{srow} \tag{193}$$

The new expression of the air flow pressure drop is obtained through the substitution of Eqs. 188 and 192 in Eq. 60

$$\Delta Pc = \sum_{srow} PD\hat{P}c_{srow} yrow_{srow} \tag{194}$$

where

$$PD\hat{P}c_{srow} = 1.1\frac{2P\hat{f}c_{srow}\left(P\hat{G}c_{srow}\right)^{2}P\hat{N}r_{srow}}{\hat{\rho}c} \tag{195}$$

The air volumetric flow rate per fan described by Eq. 66, after the discrete variables substitution, becomes

$$qfan = \sum_{srow} P\hat{q}fan_{srow} yrow_{srow} \tag{196}$$

where

$$P\hat{q}fan_{srow} = \frac{\hat{Q}}{\hat{\rho}cout\,\hat{C}pc\left(\hat{T}co-\hat{T}ci\right)}\frac{1}{P\hat{N}bay_{srow}P\hat{N}fanbay_{srow}} \tag{197}$$

The flow velocity of the fans is obtained through the substitution of Eq. 196 in Eq. 65

$$vfr = \sum_{srow} P\hat{v}fr_{srow} yrow_{srow} \tag{198}$$

where

$$P\hat{v}fr_{srow} = \frac{4\hat{Q}}{\pi\,\hat{\rho}cout\,\hat{C}pc\,(\hat{T}co - \hat{T}ci)} \frac{1}{(P\hat{D}fan_{srow})^2 P\hat{N}bay_{srow} P\hat{N}fanbay_{srow}} \quad (199)$$

Now, the total air-side pressure variation ($\Delta Pfan$) after the substitution of Eqs. 194 and 198 in Eq. 64 becomes

$$\Delta Pfan = \sum_{srow} \left[PD\hat{P}c_{srow} + \frac{\hat{\rho}c}{2} (P\hat{v}fr_{srow})^2 \right] yrow_{srow} \quad (200)$$

Finally, the total power consumption per fan is obtained through the substitution of Eqs. 196 and 200 in Eq. 71

$$Wused = \sum_{srow} P\hat{W}used_{srow} yrow_{srow} \quad (201)$$

where

$$P\hat{W}used_{srow} = \frac{1}{1000\ \eta fan\,\hat{\eta}sr\,\hat{\eta}motor} [PD\hat{P}c_{srow} P\hat{q}fan_{srow} + \frac{\hat{\rho}c}{2} (P\hat{v}fr_{srow})^2 P\hat{q}fan_{srow}] \quad (202)$$

The constraints related to the fan mechanical characteristics, obtained from the substitution of the discrete variables in Eqs. 67–69, are

$$\sum_{srow} P\hat{N}bbay_{srow}\, P\hat{D}te_{srow} P\hat{r}p_{srow} P\hat{N}tr_{srow} yrow_{srow} \geq \sum_{srow} \left(P\hat{D}fan_{srow} + 2\hat{f}d\right) yrow_{srow} \quad (203)$$

$$\sum_{srow} \left\{P\hat{D}fan_{srow} + 2\hat{f}l + 1.1\left[P\hat{D}fan_{srow}\left(P\hat{N}fanbay_{srow} - 1\right)\right]\right\} yrow_{srow} \leq \sum_{srow} P\hat{L}_{srow} yrow_{srow} \quad (204)$$

$$\frac{\pi}{4} \sum_{srow} P\hat{N}fanbay_{srow} \left(P\hat{D}fan_{srow}\right)^2 yrow_{srow} \geq 0.4 \sum_{srow} P\hat{N}bbay_{srow} P\hat{r}p_{srow} P\hat{D}te_{srow} P\hat{N}tr_{srow} P\hat{L}_{srow} yrow_{srow} \quad (205)$$

Economic model

After the substitutions of the discrete variables and the Eq. 201 in Eqs. 74–76, the capital, maintenance, and operational costs become

$$Cinv = \sum_{srow} \left(P\hat{C}he_{srow} + P\hat{C}fs_{srow}\right) yrow_{srow} \quad (206)$$

$$Cmai = \sum_{srow} \left(0.01 P\hat{C}he_{srow} + 0.03 P\hat{C}fs_{srow}\right) yrow_{srow} \quad (207)$$

$$Cop = \hat{h}op\,\hat{C}en \sum_{srow} \left(P\hat{W}used_{srow} P\hat{N}fanbay_{srow} P\hat{N}bay_{srow}\right) yrow_{srow} \quad (208)$$

where

$$P\hat{C}he_{srow} = P\hat{N}tr_{srow} P\hat{N}r_{srow} P\hat{N}bay_{srow} P\hat{N}bbay_{srow} \left\langle \left\{ 10,010 \left[P\hat{D}te_{srow}{}^2 - \left(P\hat{D}te_{srow} - 2\hat{\delta}t\right)^2 \right] + 17,193 \left[\begin{matrix} \left(P\hat{D}te_{srow} + 2P\hat{L}f_{srow}\right)^2 \\ -P\hat{D}te_{srow}{}^2 \end{matrix} \right] P\hat{N}f_{srow} P\hat{t}f_{srow} \right\} P\hat{L}_{srow} + 32.5 \right\rangle \quad (209)$$

$$P\hat{C}fs_{srow} = (1887.5 + 163.49 P\hat{D}fan_{srow}{}^2 + 281.25 P\hat{W}used_{srow}) P\hat{N}fanbay_{srow} P\hat{N}bay_{srow} \quad (210)$$

Objective function

The substitution of the Eqs. 206–208 in Eq. 77 gives the new objective function

$$TAC = \sum_{srow} \left[\begin{matrix} P\hat{C}he_{srow}\left(C\hat{R}F + 0.01\right) + P\hat{C}fs_{srow}\left(C\hat{R}F + 0.03\right) + \\ \hat{h}op\,\hat{C}en\,P\hat{W}used_{srow} P\hat{N}fanbay_{srow} P\hat{N}bay_{srow} \end{matrix} \right] yrow_{srow} \quad (211)$$

Final structure

After the application of the procedure above, the final linear problem becomes:

Min *TAC* (Eq. 211)

subjected to:

Equations 119, 148, 149, 160–162, 171, 172, 177, 178, 186, 187, and 203–205.

Convergence Acceleration

The analysis of the constraints listed above demonstrates that it is possible to use the limits imposed by some of them to accelerate the convergence through the insertion of new constraints to directly exclude solution alternatives. A similar procedure was adopted by Gonçalves et al.,[11] but keeping all of the original model constraints. Here, we explore this approach substituting the original constraints by the new ones. The following subsections present the new constraints for Alternative 3.

Hot stream Reynolds number lower bound

The extra set constraint based on Eq. 148 is

$$yrow_{srow} = 0 \quad \text{for} \quad srow \in SRehminout \quad (212)$$

The set *SRehminout* is defined from the original set of problem parameters, as follows

$$SRehminout=\left\{ srow/PRe\hat{h}_{srow} \le Re\hat{h}min-\hat{\varepsilon} \right\} \quad (213)$$

where $\hat{\varepsilon}$ is a small positive number.

L/Dti ratio lower bound

The extra set constraint based on Eq. 149 is

$$yrow_{srow}=0 \quad \text{for} \quad srow \in SLDout \quad (214)$$

The set *SLDout* is defined from the original set of problem parameters, as follows

$$SLDout=\left\{ srow/\frac{P\hat{L}_{srow}}{P\hat{D}te_{srow}-2\hat{\delta}t} \le 10-\hat{\varepsilon} \right\} \quad (215)$$

Air Reynolds number bounds

The extra set constraint based on Eq. 160 is

$$yrow_{srow}=0 \quad \text{for} \quad srow \in (SRecminout \cup SRecmaxout) \quad (216)$$

The sets *SRecminout* and *SRecmaxout* are defined from the original set of problem parameters, as follows

$$SRecminout=\left\{ srow/P\hat{R}ec_{srow} \le Re\hat{c}min-\hat{\varepsilon} \right\} \quad (217)$$

$$SRecmaxout=\left\{ srow/P\hat{R}ec_{srow} \ge Re\hat{c}max+\hat{\varepsilon} \right\} \quad (218)$$

Pitch ratio bounds

The extra set constraint based on Eq. 161 is

$$yrow_{srow}=0 \quad \text{for} \quad srow \in (Srpminout \cup Srpmaxout) \quad (219)$$

The sets *Srpminout* and *Srpmaxout* are defined from the original set of problem parameters, as follows

$$Srpminout=\left\{ srow/P\hat{D}te_{srow}P\hat{r}p_{srow} \le 0.0274-\hat{\varepsilon} \right\} \quad (220)$$

$$Srpmaxout=\left\{ srow/P\hat{D}te_{srow}P\hat{r}p_{srow} \ge 0.0986+\hat{\varepsilon} \right\} \quad (221)$$

Aot/Ar ratio bounds

The extra set constraint based on Eq. 162 is

$$yrow_{srow}=0 \quad \text{for} \quad srow \in (SADminout \cup SADmaxout) \quad (222)$$

The sets *SADminout* and *SADmaxout* are defined from the original set of problem parameters, as follows

$$SADminout=\left\{ srow/\frac{P\hat{A}ot_{srow}}{\pi P\hat{D}te_{srow}} \le 1-\hat{\varepsilon} \right\} \quad (223)$$

$$SADmaxout=\left\{ srow/\frac{P\hat{A}ot_{srow}}{\pi P\hat{D}te_{srow}} \ge 50+\hat{\varepsilon} \right\} \quad (224)$$

Lf/tf ratio lower bound

The extra set constraint based on Eq. 171 is

$$yrow_{srow}=0 \quad \text{for} \quad srow \in SLftfminout \quad (225)$$

The set *SLftfminout* is defined from the original set of problem parameters, as follows

$$SLftfminout=\left\{ srow/\frac{P\hat{L}f_{srow}}{P\hat{t}f_{srow}} \le 3-\hat{\varepsilon} \right\} \quad (226)$$

Df/Dte ratio upper bound

The extra set constraint based on Eq. 172 is

$$yrow_{srow}=0 \quad \text{for} \quad srow \in SDfDtemaxout \quad (227)$$

The set *SDfDtemaxout* is defined from the original set of problem parameters, as follows

$$SDfDtemaxout=\left\{ srow/\frac{P\hat{D}te_{srow}+2P\hat{L}f_{srow}}{P\hat{D}te_{srow}} \ge 3+\hat{\varepsilon} \right\} \quad (228)$$

Required area bound

The extra set constraint based on Eq. 177 is

$$yrow_{srow}=0 \quad \text{for} \quad srow \in SXaout \quad (229)$$

The set *SXaout* is defined from the original set of problem parameters, as follows

$$SXaout=\left\{ srow/\frac{P\hat{A}_{srow}P\hat{F}conf_{srow}}{\hat{X}a}\Delta\hat{T}lm \le \frac{\hat{Q}}{P\hat{U}_{srow}}-\hat{\varepsilon} \right\} \quad (230)$$

Spacing between the fins of adjacent tubes bound

The extra set constraint based on Eq. 178 is

$$yrow_{srow}=0 \quad \text{for} \quad srow \in SrpDfminout \quad (231)$$

The set *SrpDfminout* is defined from the original set of problem parameters, as follows

$$SrpDfminout=\{ srow/P\hat{D}te_{srow}P\hat{r}p_{srow} \le P\hat{D}te_{srow} +2P\hat{L}f_{srow}+\hat{\alpha}t-\hat{\varepsilon} \} \quad (232)$$

Hot stream pressure drop upper bound

The extra set constraint based on Eq. 186 is

$$yrow_{srow}=0 \quad \text{for} \quad srow \in SDPhmaxout \quad (233)$$

The set *SDPhmaxout* is defined from the original set of problem parameters, as follows

$$SDPhmaxout=\left\{ srow/P\hat{D}Pf_{srow}+PD\hat{P}r_{srow} \ge \Delta\hat{P}max+\hat{\varepsilon} \right\} \quad (234)$$

Hot stream flow velocity bounds

The extra set constraint based on Eq. 187 is

$$yrow_{srow}=0 \quad \text{for} \quad srow \in (Svhminout \cup Svhmaxout) \quad (235)$$

The sets *Svhminout* and *Svhmaxout* are defined from the original set of problem parameters, as follows

$$Svhminout=\left\{ srow/\frac{P\hat{G}h_{srow}}{\hat{\rho}h} \le v\hat{h}min-\hat{\varepsilon} \right\} \quad (236)$$

$$Svhmaxout=\left\{ srow/\frac{P\hat{G}h_{srow}}{\hat{\rho}h} \ge v\hat{h}max+\hat{\varepsilon} \right\} \quad (237)$$

Fans mechanical bounds

The extra set constraints based on Eqs. 203–205 are

$$yrow_{srow}=0 \quad \text{for} \quad srow \in Sfdout \tag{238}$$

$$yrow_{srow}=0 \quad \text{for} \quad srow \in Sflout \tag{239}$$

$$yrow_{srow}=0 \quad \text{for} \quad srow \in SPAfanout \tag{240}$$

The sets *Sfdout*, *Sflout*, and *SPAfanout* are defined from the original set of problem parameters, as follows

$$Sfdout=\{\, srow/P\hat{N}bbay_{srow}P\hat{D}te_{srow}P\hat{r}p_{srow}P\hat{N}tr_{srow} \le P\hat{D}fan_{srow}+2\hat{f}d-\hat{\varepsilon}\,\} \tag{241}$$

$$Sflout=\{\, srow/P\hat{D}fan_{srow}+2\hat{f}l+1.1[P\hat{D}fan_{srow}(P\hat{N}fanbay_{srow}-1)\,] \ge P\hat{L}_{srow}+\hat{\varepsilon}\,\} \tag{242}$$

$$SPAfanout=\left\{ srow/\frac{\pi}{4}P\hat{N}fanbay_{srow}\left(P\hat{D}fan_{srow}\right)^2 \le 0.4P\hat{N}bbay_{srow}P\hat{r}p_{srow}P\hat{D}te_{srow}P\hat{N}tr_{srow}P\hat{L}_{srow}-\hat{\varepsilon} \right\} \tag{243}$$

Results

Problem data

The proposed linear formulation was used to solve the air cooler design problem of the thermal task described in Table 5 associated to the parameters displayed in Table 6. The physical properties of the hot stream are listed in Table 7. This problem was originally presented in Serth[10] (Example 12.1).

The standard values of the design variables are displayed in Tables 8–10. The data of the economic model are listed in Table 11.

Model validation

To verify the modeling results, it is important to validate the model by the comparison of its outputs with data taken from the literature. The modeling proposed in this article was compared with the results reported in Serth.[10] Basically, the optimization model was run with the design variables fixed in the values from the literature data, as shown in Table 12.

The comparison of the model results is reported in Table 13, indicating a good agreement with the results provided by Serth.[10] The maximum difference obtained is 1.29% in the air-side pressure drop.

Table 5. Air Cooler Design Problem: Thermal Task

	Tube Side		Air Side	
Fluid	Hydrocarbon		Air	
Mass flow rate (kg/s)	31.5		–	
Inlet temperature (°C)	121.15		35.05	
Outlet temperature (°C)	65.65		65.65	
Fouling factor (m^2 K/W)	0.00017611		0	
Allowable pressure drop (Pa)	105,000		–	
Flow velocity bounds (m/s)	1	3	–	–
Reynolds bounds	10,000	–	1800	10^5

Table 6. Air Cooler Design Problem: Mechanical Data

Parameter	Value
$\hat{X}a$	1.1
$\hat{\delta}t$ (m)	0.002413
$\hat{\alpha}t$ (m)	0.003175
$\hat{f}d$ (m)	0.1524
$\hat{f}l$ (m)	0.1524

Table 7. Air Cooler Design Problem: Physical Properties of the Hot Stream

	Hot Stream
Density (kg/m^3)	800
Heat capacity (J/kg·K)	2303
Viscosity (Pa·s)	$5{\cdot}10^{-4}$
Thermal conductivity (W/m·K)	0.14

Table 8. Air Cooler Design Problem: Standard Values of the Discrete Design Variables

Variable	Values
Number of bays	1, 2
Number of bundles per bay	1, 2, 3
Number of fans per bay	1, 2
Number of tubes per row	35, 38, 41, 44, 47, 50, 53, 56
Pitch ratio	2, 2.5
Fan diameter (m)	1.2, 2.2, 3.2, 4.2, 5.2
Tube length (m)	4.572, 6.096, 7.315, 9.114, 10.973

Table 9. Air Cooler Design Problem: Standard Values of the Air Cooler Configuration

Number of Tube Passes	Number of Rows
1	3
1	4
1	5
1	6
3	3
4	4
5	5
6	6
2	4

Optimal solution

After the model validation, the design problem was solved in the optimization software *GAMS* using the MILP solver *CPLEX* (based on a branch-and-cut algorithm). According to the amount of standard values of the design variables shown in Tables 8–10, there are 216,000 possible design alternatives in the search space.

Table 10. Air Cooler Design Problem: Standard Values of the Finned Tubes

Outer Diameter (m)	Fin Height (m)	Number of Fins (1/m)	Fin Thickness (m)
0.0254	0.00635	275	0.000381
0.0254	0.00635	393	0.000381
0.0254	0.009525	275	0.000381
0.0254	0.009525	393	0.000381
0.0254	0.015875	393	0.000330

Table 11. Air Cooler Design Problem: Data for the Economic Model

Data	Value
Projected lifetime of the heat exchanger, $\hat{y}$ (year)	10
Annual interest rate, $\hat{i}$	0.15
Process plant time of operation, $\hat{hop}$ (h/year)	7920
Average industrial electricity price, $\hat{Cen}$ (US$/kWh)	0.0680

Table 12. Air Cooler Design Problem: Input Data for Model Verification

Variable	Values
Number of bays	1
Number of bundles per bay	1
Number of fans per bay	2
Number of tubes per row	56
Pitch ratio	2.5
Fan diameter (m)	3.2
Tube length (m)	10.973
Tube outlet diameter (m)	0.0254
Fin height (m)	0.015875
Number of fins per length (1/m)	393
Fin thickness (m)	0.000330
Number of rows	4
Number of tube passes	4

Table 13. Air Cooler Design Problem: Model Verification

	Serth[10]	Model Results	Difference (%)
Area (m^2)	4181	4212	0.74
Air-side heat-transfer coefficient (W/m^2 K)	51.78	52.23	0.85
Tube-side heat-transfer coefficient (W/m^2 K)	2385	2386	0.048
Overall heat-transfer coefficient (W/m^2 K)	25.27	25.31	0.17
Total air-side pressure drop (Pa)	122.10	123.69	1.29
Tube-side pressure drop (Pa)	100,046	100,070	0.023
Power consumption per fan (kW)	11.56	11.61	0.42

The results of the optimal design are shown in Tables 14 and 15. The performance of the optimization is illustrated in Table 16, with a comparison between the economic variables and the objective function (total annualized cost) for the heat exchanger reported in Serth[10] and the optimization results obtained by the proposed formulation for the same example.

Table 14. Air Cooler Design Problem: Optimal Design Variables

Variable	Serth[10]	Optimal Results
Number of bays	1	2
Number of bundles per bay	1	1
Number of fans per bay	2	2
Number of tubes per row	56	56
Number of tube passes	4	3
Number of rows	4	3
Pitch ratio	2.5	2.5
Fan diameter (m)	3.2	3.2
Tube length (m)	10.973	10.973
Tube outlet diameter (m)	0.0254	0.0254
Fin height (m)	0.015875	0.015875
Number of fins per length (1/m)	393	393
Fin thickness (m)	0.000330	0.000330

Table 15. Air Cooler Design Problem: Optimal Thermo-Fluidynamic Variables

Variable	Serth[10]	Optimal Results
Area (m^2)	4181	6307
Air-side Reynolds number	8115	4083
Tube-side Reynolds number	69,594	34,796
Air-side heat-transfer coefficient (W/m^2 K)	51.78	34.46
Tube-side heat-transfer coefficient (W/m^2 K)	2385	1370
Overall heat-transfer coefficient (W/m^2 K)	25.27	17.35
Total air-side pressure drop (Pa)	122.10	30.28
Tube-side pressure drop (Pa)	100,046	21,850
Power consumption per fan (kW)	11.56	1.421

Table 16. Objective Function Comparison

Variable	Serth[10]	Optimal Results
Capital cost (US$/year)	16,317	23,553
Maintenance cost (US$/year)	1092	1499
Operational cost (US$/year)	19,422	4759
Total annualized cost (US$/year)	36,830	29,811

Table 16 shows that the total annualized cost from the optimized results is about 20% smaller than the air cooler reported in Serth,[10] showing the possibility of cost savings provided by the optimization scheme compared to the feasible point search utilized by Serth,[10] which is based on an iterative procedure whose goal is to identify a feasible solution.

As can be seen in Table 14, both solutions employ tubes with the same diameter, length and finned surface. Also, both cases have only one bundle per bay. The design difference between these cases lies in the fact that the optimized solution employs two bays with three tube rows and the solution proposed by Serth[10] employs one bay with four tube rows. Consequently, the optimized solution presents a 50% larger surface (Table 15), which reflects in a higher capital cost (Table 16). The larger surface of the optimized solution is a consequence of the smaller convection coefficients (Table 15). This difference occurs due to the smaller velocities in the optimized solution, caused by the larger number of tubes per pass and the larger footprint. However, the higher capital cost associated to the optimized solution is more than compensated by the reduction of 75% of the operational cost due to the lower velocities compared to the result obtained by Serth.[10] Therefore, the proposed approach identifies an air cooler with a smaller total annualized cost, due to a better tradeoff between capital and operating costs.

Analysis of the problem dimension

Table 17 presents the problem dimension for the three alternatives described above (Table 4). It is possible to notice that the total number of binary variables increases with the aggregation level of the discrete variables. For this reason, the number of binary variables in Alternative 3 is significantly higher than in Alternatives 1 and 2. On the other hand, the use of

Table 17. Problem Dimension

	Alternative 1	Alternative 2	Alternative 3
Constraints	2,911,127	1,421,483	19
Number of binary variables	41	103	216,000
Total number of variables	308,481	242,083	216,000

Table 18. Solution Time Results

	Alternative 1	Alternative 2	Alternative 3
Computational time (s)	15,768	2146	81

additional continuous variables and constraints for conversion to a linear formulation follows an opposite trend. In fact, Alternative 3 does not need the utilization of auxiliary continuous variables (i.e., it is an ILP problem) and employs an extremely lower number of constraints in comparison to Alternatives 1 and 2.

Analysis of computational efforts

Table 18 presents the elapsed time for the solution of the problem formulation according to the three alternatives discussed above (Table 4). The objective function found in all alternatives is the same (US$29 811), since the solution is the global optimum in the three linear formulation alternatives. The computational times were measured using a computer with a processor Intel Core i7 3.40 GHz with 12.0 GB RAM memory.

The results displayed in Table 18 indicate a large reduction of the computational effort for the solution of the design problem formulated using Alternative 3 compared to the use of the other alternatives. Computational results indicate that the number of branch-and-bound nodes explored in the solution decreases from Alternative 1 to Alternative 3. Additionally, the same pattern is also verified for the solver time associated to the solution of the relaxation problems. The combined effect of the two factors results in the large reduction of the computational time observed.

Analysis of the convergence acceleration

Table 19 presents the elapsed time for the convergence acceleration procedures for the original Alternative 3 formulation. The results indicate that it is possible to reduce the computational time in about 90% when some of the original constraints are substituted by simple alternative elimination constraints. This decrease is due to the reduction of the relaxation search space obtained through the insertion of the constraints that impose the values of some sets of binaries equal to zero.

Investigation of alternative solutions

The optimization procedure can also be applied to generate alternative design solutions. After the resolution of the optimization problem, an additional constraint can be inserted into the formulation to forbid the optimal solution previously found ($y_{srow} = 0$) and the problem can be solved again to determine the air cooler design associated to the second lowest value of the objective function. The procedure can be repeated recursively a certain number of times to compose a ranking of optimal solutions. This ranking also allows an overview of how the search space is organized.

Table 19. Set Reduction Analysis Results

	Alternative 3	Gonçalves et al.[11] Proposal	Alternative Proposal
Computational time (s)	81	19	8

Table 20. Best Design Solution Alternatives

Variable	Best Solution	Second-Best Solution	Third-Best Solution
Area (m^2)	6307	3249	3307
Total power consumption (kW)	5.684	9.646	9.416
Capital cost (US$/year)	23,553	22,532	22,878
Maintenance cost (US$/year)	1499	1376	1392
Operational cost (US$/year)	4759	8075	7884
Total annualized cost (US$/year)	29,811	31,983	32,154

The results of the application of this investigation to the design example proposed here are shown in Table 20, including the three best solution alternatives. It is important to observe that the second-best and third-best solutions are not in the neighborhood of the best solution. The second-best solution and third-best solution present different balances between capital and operational costs. This scenario illustrates why traditional design procedures, based on trial and error through sequential modifications of air cooler solution candidates, are prone to be trapped in nonoptimal solutions.

Conclusions

This article presented the solution of the air cooler design problem using mathematical programming based on a linear formulation. The MILP problem allows the determination of the global optimum, differently from previous mathematical programming solutions based on local optimization.

The computational time is reduced exploring the aggregation of the discrete variables in the set of binary variables. This option has allowed a reduction of the computational time of 99.69% as compared to the time taken by the original representation of the binary variables (Alternative 3 vs. Alternative 1).

The exploration of a procedure for convergence acceleration through the substitution of some constraints allows an additional computational time reduction of 90.24% (Alternative proposal vs. Alternative 3).

Further research may involve the inclusion of additional tradeoffs in the air cooler design problem, expanding the search space.

Notation

Parameters

$\hat{C}en$ = industrial electricity price, $/kWh
$C\hat{R}F$ = capital recovery factor
$\hat{C}pc$ = air heat capacity, J/kg K
$\hat{C}ph$ = hot stream heat capacity, J/kg K
$\hat{C}r$ = parameter for calculating NTU
$\hat{F}base$ = correction factor for the unmixed–unmixed cross-flow configuration
$\hat{f}d$ = minimum distance between the fan and the bay width, m
$\hat{f}l$ = minimum distance between the fan and the bay length, m
$\hat{g}$ = gravity acceleration, m/s^2
$\hat{h}op$ = equipment hours of operation per year, h/year
$\hat{i}$ = annual interest rate
$\hat{k}c$ = air thermal conductivity, W/m K
$\hat{k}f$ = fin thermal conductivity, W/m K
$\hat{k}h$ = hot stream thermal conductivity, W/m K
$\hat{k}t$ = tube thermal conductivity, W/m K
$\hat{m}c$ = air mass flow rate, kg/s
$\hat{m}h$ = hot stream mass flow rate, kg/s
$N\hat{T}U$ = number of units of heat transfer
$\hat{P}rc$ = air Prandtl number
$\hat{P}rh$ = hot stream Prandtl number
$\hat{Q}$ = heat duty, W

$\hat{Rec}max$ = maximum allowable air-side Reynolds number
$\hat{Rec}min$ = minimum allowable air-side Reynolds number
$\hat{Reh}min$ = minimum allowable tube-side Reynolds number
$\hat{R}fc$ = air-side fouling factor, m^2 K/W
$\hat{R}fh$ = tube-side fouling factor, m^2 K/W
$\hat{T}ci$ = air inlet temperature, °C
$\hat{T}cm$ = average temperature of air, °C
$\hat{T}co$ = air outlet temperature, °C
$\hat{T}hi$ = hot stream inlet temperature, °C
$\hat{T}ho$ = hot stream outlet temperature, °C
$\hat{vh}max$ = maximum allowable tube-side flow velocity, m/s
$\hat{vh}min$ = minimum allowable tube-side flow velocity, m/s
$\hat{X}a$ = excess of area
$\hat{y}$ = projected lifetime of the heat exchanger, year
$\hat{\alpha}t$ = minimum spacing between the fins of adjacent tubes, m
$\Delta\hat{P}max$ = tube-side maximum allowable pressure drop, Pa
$\hat{\delta}t$ = tube thickness, m
$\Delta\hat{T}lm$ = log-mean temperature difference
$\hat{\varepsilon}$ = heat exchanger effectiveness
$\hat{\mu}c$ = average air viscosity, Pa s
$\hat{\mu}h$ = average hot stream viscosity, Pa s
$\hat{\eta}fan$ = fan efficiency
$\hat{\eta}motor$ = motor efficiency
$\hat{\eta}sr$ = speed reducer efficiency
$\hat{\rho}c$ = average air density, kg/m^3
$\hat{\rho}cout$ = air outlet density, kg/m^3
$\hat{\rho}h$ = average hot stream density, kg/m^3

Sets

$sconf$ = air cooler configuration, $1...sconfmax$
$sDfan$ = fan diameter, $1...sDfanmax$
sL = tube length, $1...sLmax$
$sNbay$ = number of bays, $1...sNbaymax$
$sNbbay$ = number of bundles per bay, $1...sNbbaymax$
$sNfanbay$ = number of fans per bay, $1...sNfanbaymax$
$sNtr$ = number of tubes per row, $1...sNtrmax$
srp = pitch ratio, $1...srpmax$
$stube$ = finned tube dimensions, $1...stubemax$
$srow$ = all discrete variables

Binary variables

$yconf_{sconf}$ = selection of the air cooler configuration
$yDfan_{sDfan}$ = selection of the fan diameter
yL_{sL} = selection of the tube length
$yNbay_{sNbay}$ = selection of the number of bays
$yNbbay_{sNbbay}$ = selection of the number of bundles per bay
$yNfanbay_{sNfanbay}$ = selection of the number of fans per bay
$yNtr_{sNtr}$ = selection of the number of tubes per row
yrp_{srp} = selection of the pitch ratio
$ytube_{stube}$ = selection of the finned tube dimensions
$yrow_{srow}$ = selection of all discrete variables

Discrete variables

Dte = tube outer diameter, m
$Dfan$ = fan diameter, m
F = LMTD correction factor
L = tube length, m
Lf = fin high, m
$Nbay$ = number of bays
$Nbbay$ = number of bundles per bay
Nf = number of fins per tube length, 1/m
$Nfanbay$ = number of fans per bay
Npt = number of tube passes
Nr = number of rows
Ntr = number of tubes per row
rp = pitch ratio
sf = fin spacing, m
tf = fin thickness, m

Continuous variables

A = heat transfer area, m^2
$Aface$ = total projection area of the air cooler, m^2
Aof = fins area, m^2
Aot = total finned surface area per unit length, m^2/m
Ar = outside tube bared area per tube length, m^2/m
$Areq$ = heat transfer area, m^2
Cfs = fan system investment cost, $
Che = finned tube bundle cost, $
$Cinv$ = capital cost, $/year
Cop = operational cost, $/year
$Cmai$ = yearly maintenance cost, $/year
Df = fin diameter, m
Dti = inner tube diameter, m
FAR = free-area ratio
fc = air friction factor
fh = hot stream friction factor
Gc = air mass flux, kg/m^2 s
Gh = hot stream mass flux, kg/m^2 s
h' = corrected air-side heat-transfer coefficient, W/m^2 K
hc = air heat transfer, W/m^2 K
hh = hot stream heat transfer, W/m^2 K
$Lfanp$ = distance between the fan centers, m
Lfe = corrected fin length, m
Ltp = tube pitch, m
Nuc = air Nusselt number
Nuh = hot stream Nusselt number
$qfan$ = air volumetric flow rate per fan, m^3/s
Rec = air Reynolds number
Reh = hot stream Reynolds number
TAC = total annualized cost, $
U = overall heat-transfer coefficient, W/m^2 K
vc = air flow velocity, m/s
$vcmax$ = velocity of the air stream through the minimum flow area, m/s
vfr = air velocity through the fans, m/s
W = bundle width, m
$Wused$ = power consumption per fan, kW
ΔPc = air-side pressure drop across the air cooler, Pa
ΔPf = pressure drop caused by the fluid flow in the tubes, Pa
$\Delta Pfan$ = total air-side pressure drop, Pa
ΔPh = tube-side pressure drop, Pa
ΔPr = heads pressure drop, Pa
ηf = fin efficiency
ηt = overall efficiency of the finned surface

Literature Cited

1. Singham JR. Cooling towers. In: Schlünder, EU, editor. *Heat Exchanger Design Handbook*. New York: Hemisphere Publishing Corporation, 1983.
2. Dai A. Increasing drought under global warming in observations and models. *Nat Clim Change*. 2013;3:52–58.
3. Jegede FO, Polley GT. Optimum heat exchanger design. *Chem Eng Res Des*. 1992;70(A2):133–141.
4. Doodman AR, Fesanghary M, Hosseini R. A robust stochastic approach for design optimization of air cooled heat exchangers. *Appl Energy*. 2009;86:1240–1245.
5. Karami A, Rezaei E, Shahhosseni M, Aghakhani M. Optimization of heat transfer in an air cooler equipped with classic twisted tape inserts using imperialist competitive algorithm. *Exp Therm Fluid Sci*. 2012;38:195–200.
6. Rezaei E, Karami A, Shahhosseni M, Aghakhani M. The optimization of thermal performance of an air cooler equipped with butterfly inserts by the use of imperialist competitive algorithm. *Heat Transf-Asian Res*. 2012;41:214–226.
7. Kashani AHA, Maddahi A, Hajabdollahi H. Thermal-economic optimization of an air-cooled heat exchanger unit. *Appl Therm Eng*. 2013;54:43–55.
8. González MT, Petracci NC, Urbicain MJ. Air-cooled heat exchanger design using successive quadratic programming (SQP). *Heat Transfer Eng*. 2001;22:11–16.
9. Manassaldi JI, Scenna NJ, Mussati SF. Optimization mathematical model for the detailed design of air cooled heat exchangers. *Energy*. 2014;64:734–746.
10. Serth RW. *Process Heat Transfer: Principles and Applications*. Amsterdam: Elsevier, 2007.
11. Gonçalves CO, Costa ALH, Bagajewicz MJ. Shell and tube heat exchanger design using mixed-integer linear programming. *AIChE J*. 2017;63:1907–1922.
12. Gonçalves CO, Costa ALH, Bagajewicz MJ. Alternative Mixed-integer linear programming formulations for shell and tube heat exchanger optimal design. *Ind Eng Chem Res*. 2017;56:5970–5979.
13. Cao E. *Heat Transfer in Process Engineering*. New York: McGraw-Hill, 2010.

14. Saunders EAD. *Heat Exchangers: Selection, Design and Construction*. New York: John Wiley & Sons, 1988.
15. Shah RK, Sekulic DP. *Fundamentals of Heat Exchanger Design*. New York: John Wiley & Sons Inc., 2003.
16. Conradie AE, Buys JD, Kröger DG. Performance optimization of dry-cooling systems for power plants through SQP methods. *Appl Therm Eng*. 1998;18:25–45.

Manuscript received Jan. 30, 2017, and revision received June 1, 2017.